Optimal spatio-temporal filter for the reduction of crosstalk in surface electromyogram

Journal of Neural Engineering

Optimal Spatio-Temporal Filter for the Reduction of Crosstalk in Surface Electromyogram

Luca Mesin[1]

[1] *Mathematical Biology and Physiology, Dipartimento di Elettronica e Telecomunicazioni, Politecnico di Torino, Corso Duca degli Abruzzi 24, 10129, Turin, Italy*

Keywords: Surface EMG, Crosstalk, Spatial Filter

Corresponding author:

Luca Mesin, Ph.D.

Department of Electronics and Telecommunications, Politecnico di Torino, Corso Duca degli Abruzzi 24, Torino, 10129 ITALY

Tel. 0039-0110904085 Fax. 0039-0110904099 e-mail: luca.mesin@polito.it

Abstract

Objective. Crosstalk can pose limitations to the applications of surface electromyogram (EMG). Its reduction can help in the identification of the activity of specific muscles. The selectivity of different spatial filters was tested in the literature both in simulations and experiments: their performances are affected by many factors (e.g., anatomy, conduction properties of the tissues and dimension/location of the electrodes); moreover, they reduce crosstalk by decreasing the detection volume, recording data that represent only the activity of a small portion of the muscle of interest. In this study, an alternative idea is proposed, based on a spatio-temporal filter. *Approach.* An adaptive method is applied, which filters both in time and among different channels, providing a signal that maximally preserves the energy of the EMG of interest and discards that of nearby muscles (increasing the signal to crosstalk ratio, SCR). *Main results*. Tests with simulations and experimental data show an average increase of the SCR of about 2 dB with respect to the single or double differential data processed by the filter. This allows to reduce the bias induced by crosstalk in conduction velocity and force estimation. *Significance.* The method can be applied to few channels, so that it is useful in applicative studies (e.g., clinics, gate analysis, rehabilitation protocols with EMG biofeedback and prosthesis control) where limited and not selective information is usually available.

Abbreviations

BCI	brain computer interface
CV	muscle fiber conduction velocity
DD	double differential filter
ECR	extensor carpi radialis
ECU	extensor carpi ulnaris
EDC	extensor digitorum communis
EEG	electroencephalogram
EMG	electromyogram
FR	firing rate
IED	inter-electrode distance
IZ	innervation zone
KKT	Karush-Kuhn-Tucker
MU	motor unit

MUAP	motor unit action potential
MVC	maximum voluntary contraction
OSF	optimal spatial filter
OSTF	optimal spatio-temporal filter
RMS	root mean square
SCR	signal to crosstalk ratio
SD	single differential filter
SFAP	single fiber action potentials
SNR	signal to noise ratio

Introduction

Crosstalk in surface electromyogram (EMG) is the signal recorded over the skin above a muscle, but produced by another. It limits the reliability of EMG in many applications. For example, it may interfere in studies that are focused on muscle coordination [1], gait analysis [2], ergonomics for task evaluation [3], prosthetic control [4] and reflexes [5].

Many studies investigated the effect of crosstalk in different simulated [6-10] or experimental [11-15] settings and proposed methods to quantify or to reduce it. The following main indications are provided by the literature.

- Crosstalk increases for a thicker subcutaneous layer [16].
- It largely depends on electrode location [17].
- It cannot be removed by temporal high-pass filters, as it is mostly related to non-propagating components [18].
- It can be reduced by selective spatial filters [11,13], but the optimal configuration depends on anatomical and physical parameters (studied in many simulation studies, e.g., [6-10]).
- It cannot be quantified studying the cross-correlation between the EMGs recorded over the two muscles involved [19].
- It can be studied by sophisticated techniques which are difficult to employ in applications, for example the followings:

1. under the hypotheses that the recorded data are linear instantaneous mixtures of independent signals produced by the investigated muscles (sources) and that the number of detected signals is larger than that of the muscles, an advanced blind source separation technique was applied to time frequency representations of the data to

remove crosstalk [14]; however, the algorithm cannot be easily integrated in real time applications, as the mixing matrix changes in time and should be updated processing the data which are acquired; moreover, the assumptions limit the applications to small, superficial muscles which are close to each other (to reduce the effect of the volume conductor, mostly neglected due to the assumption of linear instantaneous mixture) which are not synergic (as a possible common drive would violate the assumption of independence of the sources);

2. using sophisticated inverse methods (estimating the location of active MUs) applied to data recorded with high-density systems, crosstalk can be possibly estimated and in part removed (potential application suggested on the basis of simulations, but still to be tested on experiments [20]).

The main idea proposed in the literature to reduce crosstalk for application studies is that of using selective filters with a small detection volume on the muscle of interest. However, in this way, to remove the potential coming from the nearby muscles, also most of the EMG produced by the muscle under investigation is discarded. This could be a problem if the activity of the motor units (MU) in the small detection volume considered is not representative of the whole muscle. Moreover, selective filters could be not available for many applications in which a few, large electrodes are commonly used.

Here, a different approach is considered, based on the following principles:

1. a filter is designed adapting to the considered condition (depending on anatomy, conductivity of the volume conductor, electrode type and location, etc.);
2. the EMG of the muscle of interest should be retained and the one coming from nearby muscles should be reduced as much as possible;
3. the method should be simple and stable in order to be feasible for applications (i.e., it should work in real time and also considering simple experimental protocols using a few not selective detection channels).

In the following sections, the theory of the method is introduced and then the filter performances are assessed using simulations and experimental data.

Methods

Selection of the optimal filter

The filter coefficients are selected on the basis of a portion of the data, i.e., the training set, corresponding to selective contractions of specific muscles. Different portions of the data are

identified as either ‘signal’ or ‘crosstalk’ epochs. ‘Signal’ epochs are the portions of EMG corresponding to the activity of the muscle of interest. They are indicated with $S_i(t)$ in the following, where the subscript $i = 1,\ldots, M$ indicates the i^{th} EMG channel and time t indicates the samples of concatenated epochs, possibly not consecutive, in which the muscle of interest is active. The rest of the data (reflecting either rest or selective contraction of other muscles) was considered as ‘crosstalk’ and indicated by $C_i(t)$.

An Optimal Spatial Filter (OSF, discussed in [21] in the context of brain computer interface, BCI) can be developed by selecting the weights w_i of a linear combination of data from different channels in order to increase the signal to crosstalk ratio (SCR)

$$SCR = 10\log_{10}\frac{\left\|\sum_{i=1}^{M} w_i S_i(t)\right\|_2^2}{\left\|\sum_{i=1}^{M} w_i C_i(t)\right\|_2^2} \tag{1}$$

under the hypothesis that the sum of the weights is zero. This problem was approximately solved numerically in [21], but the correct solution can also be found analytically as follows. The common mode can be removed from monopolar data by subtracting the mean over the channels as a preliminary step. If the considered data $S_i(t)$ and $C_i(t)$ were detected by spatial filters like single or double differential (SD and DD, respectively), the common mode was already removed, so that this preliminary step can be avoided. Then, the SCR can be maximized as follows. As the logarithmic function is monotone increasing, its maximum can be obtained maximizing its argument, which can be rewritten as follows

$$J(\vec{w}) = \frac{\left\|\sum_{i=1}^{M} w_i S_i(t)\right\|_2^2}{\left\|\sum_{i=1}^{M} w_i C_i(t)\right\|_2^2} = \frac{\vec{w}^T \vec{S}^T \vec{S}\vec{w}}{\vec{w}^T \vec{C}^T \vec{C}\vec{w}} = \frac{\vec{w}^T R_S \vec{w}}{\vec{w}^T R_C \vec{w}} \tag{2}$$

where $J(\vec{w})$ is the functional to be optimized (depending on the vector of the weights $\vec{w}$) and R_S and R_C are the autocorrelation matrices of the signal and of the crosstalk, respectively.

Notice that the optimization functional $J(\vec{w})$ is invariant if the vector $\vec{w}$ is scaled: for this reason, the maximization of $J(\vec{w})$ is equivalent to the following constrained optimization problem (which is found in the theory of Linear Discriminant Analysis [22])

$$\max_{\vec{w}} \ \frac{1}{2}\vec{w}^T R_S \vec{w} \quad \text{such that} \quad \vec{w}^T R_C \vec{w} = 1 \tag{4}$$

The above problem can be solved studying the following Lagrangian

$$L_P = \frac{1}{2}\vec{w}^T R_S \vec{w} + \frac{1}{2}\lambda(1 - \vec{w}^T R_C \vec{w}) \tag{5}$$

Based on Karush-Kuhn-Tucker (KKT) conditions [23], the following equation must be satisfied

$$R_S \vec{w} = \lambda R_C \vec{w} \qquad \Rightarrow \qquad R_C^{-1} R_S \vec{w} = \lambda \vec{w} \tag{6}$$

This is an eigenvalue problem. The matrix $R_C^{-1} R_S$ is not symmetric, but a change of variables can be used to obtain a problem involving a symmetric and positive matrix. Indeed, considering that R_S is symmetric positive definite, the following vector is introduced $\vec{v} = R_S^{1/2}\vec{w}$, obtaining

$$R_S^{1/2} R_C^{-1} R_S^{1/2} \vec{v} = \lambda \vec{v} \tag{7}$$

The matrix $R_S^{1/2} R_C^{-1} R_S^{1/2}$ is symmetric and positive definite, so that its eigenvalues $\{\lambda_k\}$ are positive and the eigenvectors $\{\vec{v}_k\}$ are orthogonal. They correspond to directions of projections $\vec{w}_k = R_S^{-1/2}\vec{v}_k$. Considering such directions, the optimization functional becomes

$$J(\vec{w}_k) = \frac{\vec{w}_k{}^T R_S \vec{w}_k}{\vec{w}_k{}^T R_C \vec{w}_k} = \lambda_k \tag{8}$$

as $\vec{w}_k{}^T R_S \vec{w}_k = 1$ and $\vec{w}_k{}^T R_C \vec{w}_k = 1/\lambda_k$. Thus, the weights corresponding to a maximal SCR correspond to the eigenvector associated to the largest eigenvalue.

The OSF can be generalized considering also past values of the EMG data to increase further the SCR. In this way, the data are both filtered in time and space, obtaining the Optimal Spatio-Temporal Filter (OSTF). Specifically, the objective of the OSTF is the selection of the weights of a linear combination of present and past samples of the EMGs in order to increase the SCR. The delay between subsequent samples and the order of the temporal filters are two parameters that can be tuned, e.g., by improving the performances on a validation set. In this study, the delay was 1 sample. Some tests were performed also with a larger delay, usually obtaining improved performances (but sometimes giving overfitting of training data, with problems of generalization to test data; specifically, the SCR was a bit lower than that of classical filters when the amount of crosstalk was already small).

Consider that the delayed data have a high mutual correlation which reflects in a high condition number of the autocorrelation matrices R_S and R_C, mainly in the case in which the

delay is small and the length of the temporal filter is quite large. For this reason, the autocorrelation matrices were regularized as follows

$$\hat{R}_S = R_S + 10^{-15}\lambda^S_{\max} I \qquad \hat{R}_C = R_C + 10^{-15}\lambda^C_{\max} I \tag{9}$$

where I is the identity matrix and $\lambda^S_{\max}$ and $\lambda^C_{\max}$ are the maximum eigenvalues of R_S and R_C, respectively. Notice that the maximum possible conditional number of the regularized autocorrelation matrices $\hat{R}_S$ and $\hat{R}_C$ is in the order of 10^{15}.

The filtered data is called surrogate channel in the following.

Simulated signals

The cylindrical model proposed in [24] was used to simulate single fiber action potentials (SFAP) from two muscles. The properties of the volume conductor and of the simulated muscles are indicated in Figure 1. The skin over the muscles was covered by a 2D grid of square electrodes (surface 1 mm^2) with inter-electrode distance (IED) of 5 mm, with 3 parallel arrays of 5 electrodes aligned to the fibers. Monopolar SFAPs were simulated for fibers with length and location of IZ chosen randomly with a range of variation of 10 mm, as indicated in 1C. Then a few electrodes were used to simulate the acquisition by SD or DD channels with different IEDs. The fibers were simulated with a density of 20/mm^2. This is about the density of fibers of a MU, an order of magnitude lower than the density of fibers in the muscle [25]: this introduces an approximation, as the same fibers were included in different MUs with superimposed territory [25]. The number of fibers per MU was exponentially distributed in the range 15 – 300. The total number of simulated MUs for each of the two muscles was 200. Their location was random, uniformly distributed within the simulated muscles. The fibers closest to the center of a MU were selected to belong to it and the corresponding SFAPs were added up to simulate the motor unit action potential (MUAP). MU conduction velocity (CV) was chosen with a Gaussian distribution with mean 4 m/s and standard deviation 0.3 m/s (CV values reduced of 20% were also used to simulate peripheral fatigue, as indicated in the Results section). CV values were assigned in agreement to the size principle [26].

Interference signals were simulated according to [25], with range of recruitment thresholds equal to 60% of the maximal voluntary contraction (MVC), range of the firing rate (FR) 8-30 Hz (with linear increase with the force level with slope of 1 Hz per 1% MVC, after recruitment of the MU and until the upper limit of the FR) and 10% random (Gaussian) variability of the inter-spike interval (i.e., a random jitter was introduced with Gaussian distribution with zero mean and standard deviation equal to 10% of the mean inter-spike

interval). Signals corresponding to force levels of 5, 10, 20, 40, 60 and 80% of the MVC were generated. Epochs of 1 s duration with selective contractions at different levels of each muscle were concatenated to form the training set. Different test signals were then generated, considering different contraction levels of the muscles; moreover, different problems in the training and test data were included (see the Results section for details). SD and DD channels placed over the simulated muscles were used as input data to which the OSTF was applied. Signals were corrupted by additive white Gaussian noise low-pass filtered with cutoff 500 Hz (Chebyshev Type II filter of order 6 with 20 dB attenuation in the stop-band, used in both directions to remove the phase). Additional tests were also performed on monopolar signals from the same electrodes used to record either the SD or the DD channels (Supplementary Material). The SCRs of SD or DD channels placed over the muscle of interest were considered for comparison.

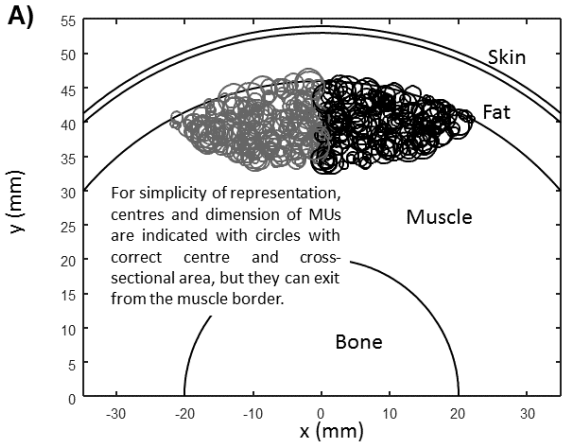

Tissue	Thickness (mm)	Conductivity (S/m)
Skin	1	$50 \cdot 10^{-2}$
Fat	3 or 7	$5 \cdot 10^{-2}$
Muscle	26	$5 \cdot 10^{-2}$ (longitudinal) $1 \cdot 10^{-2}$ (transversal)
Bone	20 (radius)	$2 \cdot 10^{-2}$

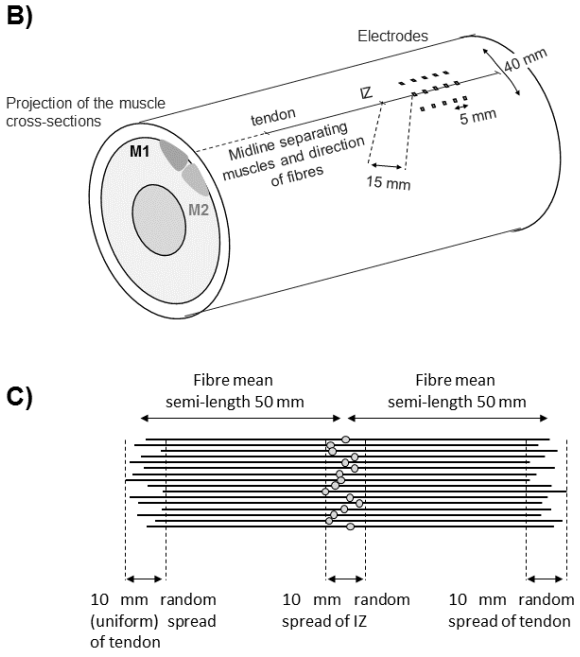

Figure 1. Simulation model. A) Section of the cylindrical volume conductor and indication of parameters. Sizes of MUs in the two simulated muscles (M1 and M2) are also shown. B) Three dimensional representation of the volume conductor, with indication of the simulated electrode grid: monopolar EMGs were simulated, then different electrodes were used to obtain single and double differential signals with different inter-electrode distances (IED). C) Fiber endings and innervation zones (IZ) were simulated with some spread (uniform distribution).

Experimental signals

Four healthy male volunteers (mean ± standard deviation: age 20.2±5.2 years, height 172±4 cm, weight 71±3 kg) participated in the study. Data were recorded in accordance with the

Declaration of Helsinki. EMG were detected with three linear adhesive arrays of 8 electrodes (AgCl) with IED of 5 mm (LISiN-SPES Medica, Battipaglia, Salerno, Italy, pat. No. GE2001A000086), in SD configuration. Each array provided 7 SD signals. The arrays were connected to two 16-channel surface EMG amplifiers (LISiN-Prima Biomedical & Sport; one amplifier was used for the first 2 electrode arrays, the other for the third array). The signals were amplified, band-pass filtered (-3dB bandwidth, 10–500 Hz), sampled at 2048 Hz, and converted in digital form with a resolution of 12-bit. The torque exerted by the subject was measured in two orthogonal directions, using a biomechanical amplifier connected to two load cells (bandwidth 0-60 Hz, sampling frequency 200 Hz). A representation of the experimental protocol and data is provided in Figure 6.

EMGs were acquired during isometric contractions at different effort levels of two extensors of the wrist: the Extensor Carpi Radialis (ECR, which is an extensor of the wrist which also abducts the hand) and the Extensor Carpi Ulnaris (ECU, which is a forearm muscle extending and adducting the wrist). Moreover, the activity of the Extensor Digitorum Communis (EDC) was also monitored, to ensure that its contribution was low. The three muscles were identified by palpation. Before placement of the arrays over them, the skin was slightly abraded with abrasive paste.

A biofeedback developed in Labview© (National Instruments) was used to provide to the subject information about the selectivity of a movement. Specifically, the amplitude of the EMG (in terms of root mean square value, RMS) recorded over each muscle was displayed. Moreover, measuring the two orthogonal components of the torque, the direction of the effort was estimated and shown. An index of selectivity was computed as the ratio between the RMS of the signal recorded over the muscle of interest and the sum of the RMSs of the EMGs taken over the other two muscles. The direction related to the maximally selective contraction of a muscle was determined in a training phase and then provided to the subject as a guide to help him to produce a selective contraction.

The protocol consisted in recording EMG during selective contractions of ECR and ECU at different force levels (in the range 10-80% of MVC, with step 10%; executed in random order, repeated twice, for a total of 16 contractions) after measuring the MVC (maximum among three attempts).

Different data were obtained combining the recorded SD signals and were then processed by the OSTF: SD channels with detection point in the center of the arrays over each muscle and IED of 5, 15, 25 or 35 mm; DD channels with detection point on the fifth electrodes of the arrays (first electrode proximal) and IED of 5, 10 or 15 mm. The OSTF was trained on the

first 4 contractions and then applied to the others, considered as test data (quasi-real time approach [21,27,28]). Not selective contractions were identified as the ones for which the RMS over the EDC was at least the 25% larger than that over the others and were removed from the test set. About 30% of data was removed, as the contractions did not pass this criterion of selectivity; moreover, one contraction was removed, as an important artifact was present, due to the detachment of one electrode.

Results

Figure 2 shows an example of application to simulated signals. Training data were obtained by an alternative selective activation of duration of 1 s of either of the two muscles with force levels of 20, 40, 60 or 80% MVC. Test data were obtained considering again the same activation protocol, but with each contraction lasting 5 s. Noisy SD and DD channels (additive Gaussian white noise filtered at 500 Hz with signal to noise ratio, SNR, equal to 15 dB) were detected from electrodes aligned to the muscle fibers, with IED 5 mm. Each channel was located over one of the two muscles, with a distance of 20 mm between the centers of the spatial filters and the midline between the two muscles. Surrogate signals were obtained applying the OSTF either to the SD or to the DD data. Notice that the SCR is larger for the surrogate channel than for the classical spatial filters. The order of the temporal filter was 5, as for all the tests that follow. This low order allows to get stable results also in the case of problems in the training and test sets, considered in the following. The selected temporal filters are not simple to interpret, as their outputs are also combined (performing a spatial filter) in order to get the surrogate. However, some considerations can be given: the temporal filters applied to both the SD and DD channels had stop-band transfer functions, attenuating frequency contributions in the range of either 250-450 Hz (channel above the muscle of interest, which has most of the power below 250 Hz) or 150-250 Hz (channel above the other muscle); notice that most of the energy contribution of crosstalk in the channel above the muscle of interest was found for frequencies lower than about 100 Hz, so that the temporal filter applied to the other channel appears to have the role of estimating the crosstalk to be subtracted from the first one.

Notice that, in the ideal conditions shown in Figure 2, stable results with larger SCR were obtained with filters of higher orders: for example, with order 50, the SCRs were over 16 and 19 dB, using SD and DD channels, respectively. These SCRs are even greater than the SNR of the data due to the additive noise: this is possible as the temporal filters of the OSTF in this case have a band-pass transfer function (with main bandwidth between 80 and 180 Hz, with

some differences among channels) that removes part of the noise (still preserving most of the signal).

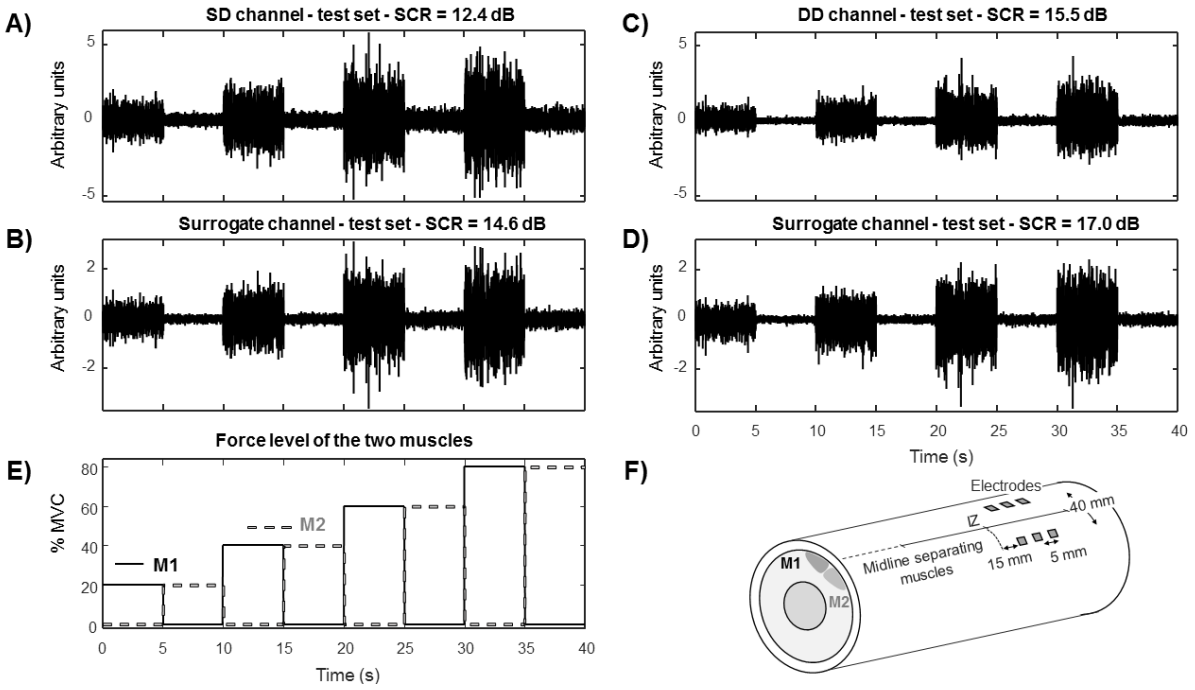

Figure 2. Example of single differential (SD), double differential (DD) and surrogate data (volume conductor with thickness of fat layer equal to 7 mm; noise with SNR of 15 dB was added to SD and DD, before computing surrogates). Training set was equivalent to the test dataset (it was only 5 times shorter). A) SD data detected over muscle M1, with indication of the signal to crosstalk ratio (SCR); channels closer to the IZ were considered. B) Surrogate signal obtained from two SD channels placed over the two muscles, with order for the temporal filter equal to 5. C) DD data detected over M1. D) Surrogate signal obtained considering the two DD channels placed over the two muscles. E) Force level of the two muscles for the test dataset. F) Representation of the volume conductor and electrodes considered.

Figure 3 shows some examples of results obtained in equivalent conditions as in Figure 2, but considering some problems in the training or in the test data. In Figure 3A, the effect of limited information in the training set is considered: only contraction levels of 20 and 40% MVC were considered in the training set. As the recruitment threshold of the largest MU was 60% MVC, only some MUs were active in the data used for training, expecting to get reduced performances when the method is applied on test data, as additional MUs contributed to them. In Figure 3B, in addition to the limited information, a further problem was considered: contractions used for the training were not perfectly selective, but a contraction with level of either 5 or 10% MVC of the muscle assumed to be silent was included. Specifically, a contraction of either 20 or 40% MVC of muscle 1 was added to a contraction of muscle 2 at either 5 or 10% MVC, respectively, during the assumed selective contraction of the first

muscle; when measuring crosstalk over muscle 1, the opposite was simulated, so that muscle 1 was not silent, but contracted at either 5 or 10% MVC, during a contraction of muscle 2 at 20 or 40% MVC, respectively. Figure 3C includes a further problem, in addition to the previous ones: the muscle is fatigued during the test, with a reduction of muscle fiber CV of 20%.

Figure 4 shows a summary of the results of many simulations. The following parameters were changed across different simulations:

1. fat layer thickness (either 3 or 7 mm);
2. IED (5 or 10 mm);
3. SNR of the SD or DD channels (considering additive colored Gaussian noise with bandwidth 0-500 Hz, as described in the Methods section, with SNR of either 10 or 20 dB);
4. number of spatial filters, either 2 or 3, with the latter case indicating that an additional channel was located over the midline between the two muscles (the spatial filters over the muscles were always at 20 mm from the midline, see Figure 1).

All cases discussed above (and shown in Figure 2 and 3) were considered: ideal condition in which training data included perfectly selective contractions at different force levels ranging among 20 to 80% MVC and test data were generated considering the same MUAPs as for the training data; limited information in the training data (up to a force level of 40% MVC); limited information and not selective contractions used for the training data; same training data as in the latter case, but considering test data showing myoelectric manifestation of peripheral fatigue. General results are as expected (all following indications are statistically significant for Wilcoxon signed rank test, with $p<0.01$):

- mean performances of OSTF decrease (i.e., a lower SCR is obtained) when problems on training or test data are included;
- performances of all methods decrease by increasing the fat layer thickness and by decreasing the SNR;
- performances of OSTF increase when including an additional channel over the midline separating the two muscles;
- performances increase when IED is smaller, i.e., when SD and DD filters are more selective.

As shown in 4E, the performances of surrogates were always greater than those of SD and DD filters, with a median gain that was between about 2 and 2.8 dB, in different conditions.

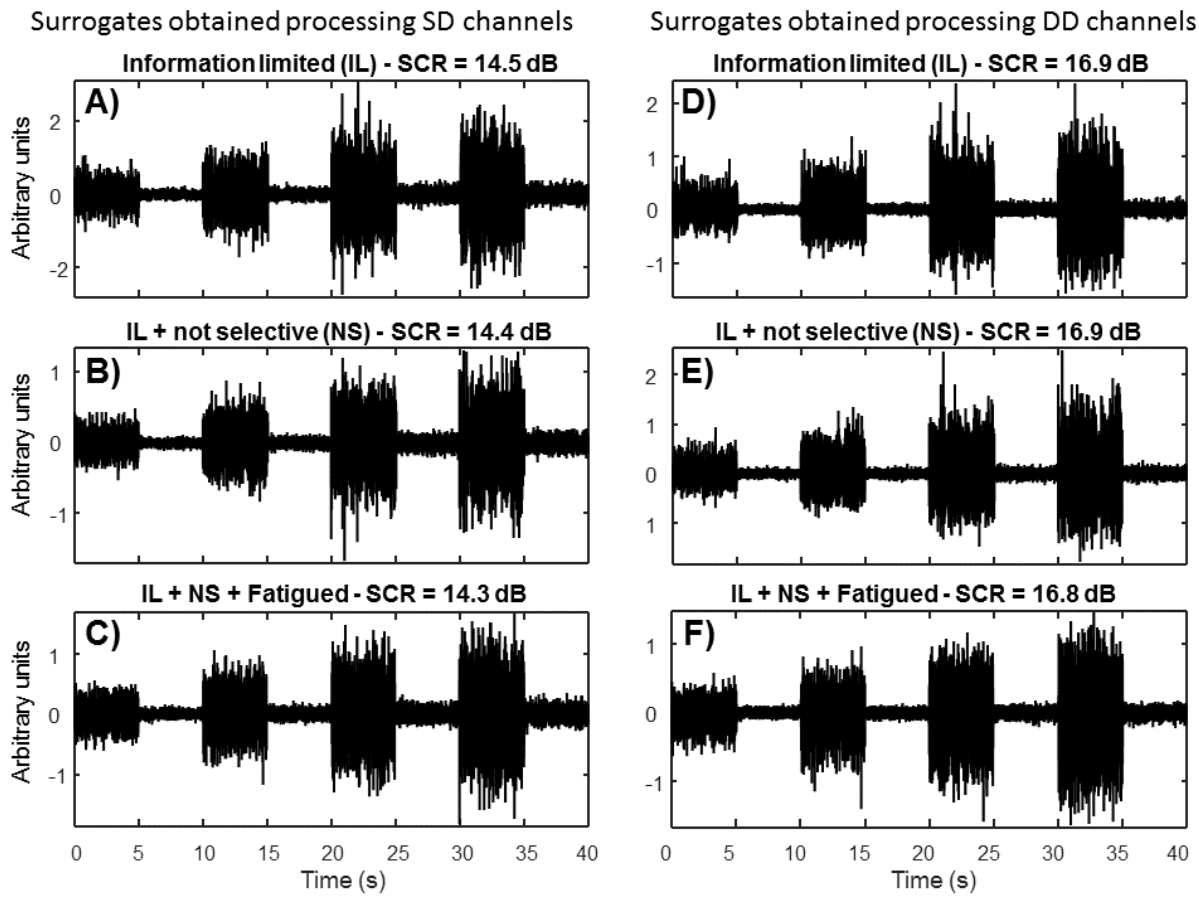

Figure 3. Examples of surrogate data (with order of the temporal filter equal to 5) obtained considering the same configuration as in Figure 2, but including different problems. A), B), C) SD data are considered (as in 2B). D), E), F) DD signals are considered (as in 2D). A), D) Only force levels of 20 and 40% of maximal voluntary contraction (MVC) were considered for the training set. B), E) In addition to the limited information, in the training set the contractions were not selective, but, during the contraction at 20 and 40% MVC, they included a contraction of the other muscle at 5 and 10% MVC, respectively. C), F) In addition to the previous problems, the test data showed myoelectric fatigue (20% reduction of muscle fiber conduction velocity).

Figure 5 shows applications to CV and force level estimation. Both estimates are biased by crosstalk, mainly when the muscle of interest has a low level of contraction. The simulated force level of the muscle of interest was between 0 and 20% MVC, whereas that of the other muscle ranged between 20 and 80% MVC. In the training set, the muscles were activated selectively, whereas the two muscles were active together during the test (with force levels indicated in 5I). CV was computed with the spectral matching algorithm [29], considering either a pair of SD or DD filters, aligned to the muscle fibers and placed over the muscle of interest (at 20 mm from the midline between the two muscles), or using the OSTF (3 arrays were used, 1 over each muscle and 1 on the midline separating them). EMGs from channels closer to the IZ were used for training the OSTF; it was then applied to the test data from

channels either closer to the IZ or to the tendon, obtaining the ideally delayed signals to which the spectral matching algorithm was applied. The estimates were computed from data either including or excluding crosstalk, in order to compare the estimates of CV when crosstalk was present or absent. Moreover, the mean CV of active MUs of the muscle of interest (weighted by the sizes of the MUs) was computed as a further reference. CV values estimated when the muscle of interest was not contracted (left portions of A-F) are not reliable. The other values are affected by a larger bias when the force level of the muscle of interest is lower and that of the other muscle is greater. The OSTF allows to get a better estimate of CV, both when compared to the mean CV of active MUs and to the one computed from crosstalk-free data.

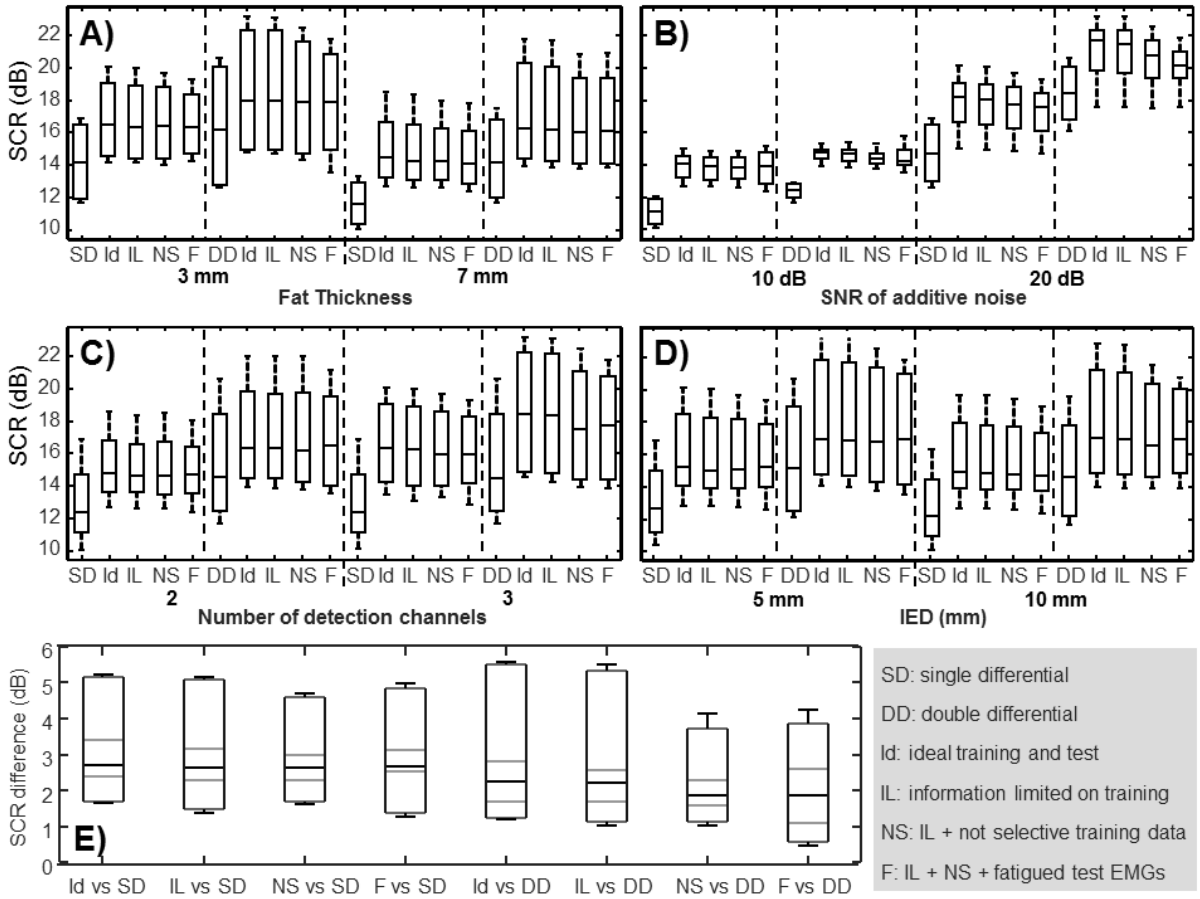

Figure 4. Summary of many simulations (order of the temporal filter equal to 5). The following parameters were changed across simulations: fat layer thickness (either 3 or 7 mm), IED (5 or 10 mm), SNR (10 or 20 dB), number of spatial filters (either 2 or 3, with 3 indicating that electrodes were placed also over the midline between the two muscles). Ten realizations of noise were considered for each simulated condition. SD or DD channels were simulated. Surrogates were computed considering either SD or DD data, in either ideal conditions (training and test data with equivalent properties) or including the problems also shown in Figure 3. Data were pooled, showing the effect of different parameters (median, quartiles and range): A) fat thickness, B) noise level, C) number of channels, D) IED. E) Distribution of differences between SCR obtained using surrogates and either SD or DD (median, percentiles of percentages 5, 25, 75, 95, range).

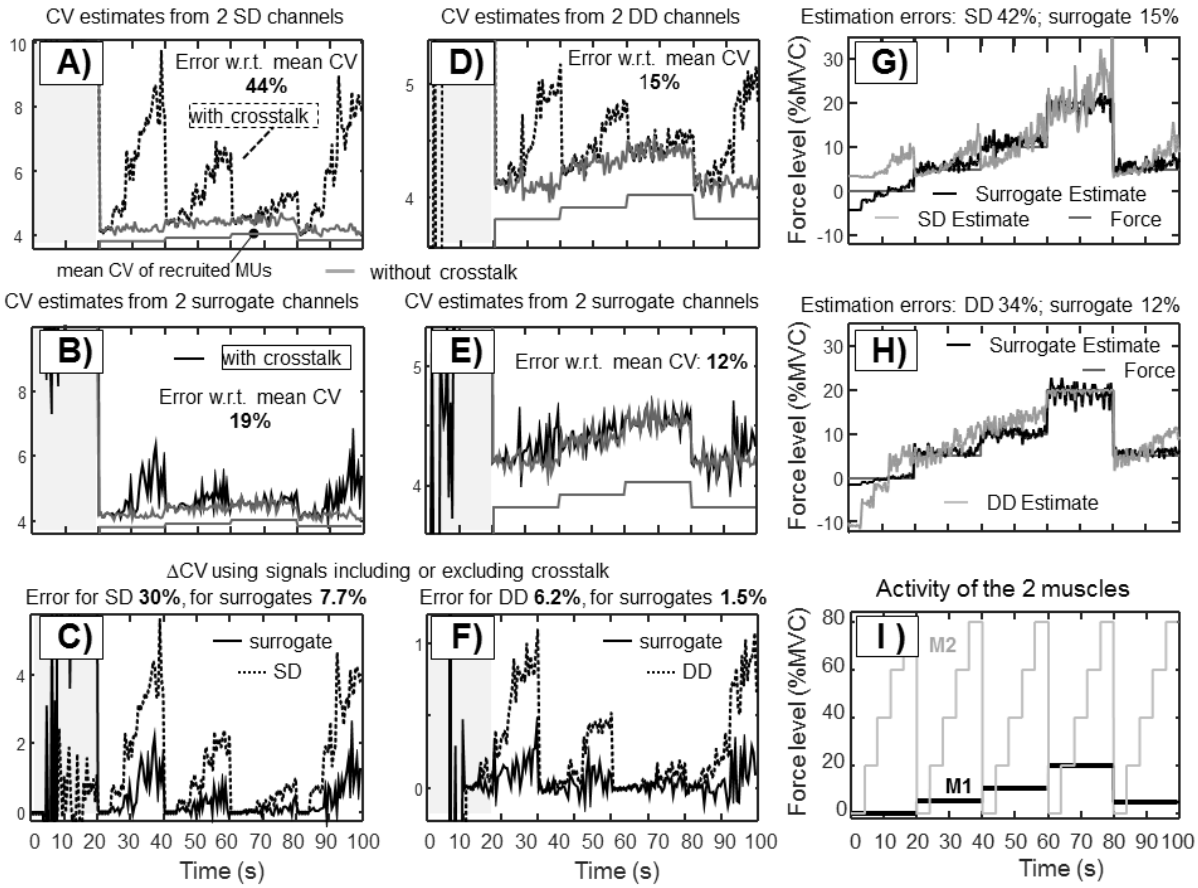

Figure 5. Examples of applications to simulated data (with order of the temporal filter equal to 5): A)-F) CV estimation; G), H) force level estimation. A) CV estimation using epochs of 0.5 s of two SD channels from 3 electrodes aligned to the fibers, with 5 mm of IED and placed over the first muscle (M1), at 20 mm from the midline separating the two muscles. Crosstalk was either included or not. B) Same as A), but considering surrogates computed from an ideal training set, using 3 SD channels (the first array as in A, the second over the midline, the third over M2, symmetrical to the first with respect to the midline). C) Difference between the CV computed either including or excluding crosstalk. D) Same as A), but considering DD channels. E) Same as B), but using DD channels to compute the surrogate. F) Same as C), but using data shown in D) and E). G) Estimation of force level using the envelope of SD and corresponding surrogate, with a quadratic model. H) Estimation of force level using the envelope of DD and surrogate. I) Force levels of the two muscles over time.

Force estimation is considered in Figures 5G-H, using the same signals as before (channels closest to the IZ). Given the training signal of interest (using either SD or DD channels over the muscle, or the two surrogates from the OSTFs), the envelope was computed (low-pass filtered absolute value, with cutoff frequency of 3 Hz, Chebychev type II filter of order 6, processing in both directions to remove the phase). Then, a quadratic model was fit to training data to estimate the force level as a function of the envelope. The model was then applied to the test data. Notice that SD and DD show a large bias, due to the activity of the other muscle.

Using the OSTF, the content of crosstalk was reduced, so that force estimation was more precise.

Figure 6 shows the experimental setup (mechanical brace and investigated muscles) and protocol. The contractions of ECR and ECU muscles were investigated, whereas EDC was monitored to check that its contribution was low. Some examples of test data from a subject are also shown: the SCR were higher when considering the surrogate signals obtained using the OSTFs instead of the SD channels recorded over the two muscles. The order of the temporal filter of the OSTF was again 5 for the experimental data, as in the tests on simulations shown before.

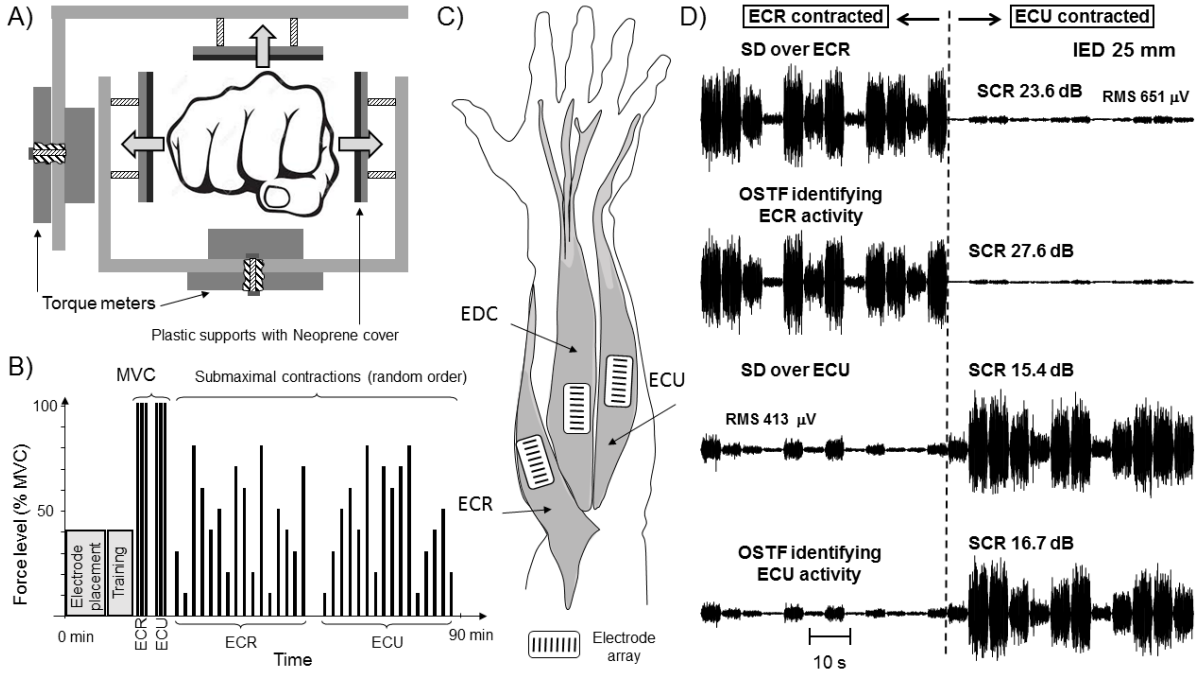

Figure 6. Test on experimental data. A) Configuration of the mechanical brace, front view. The torque meters provide the direction and intensity of the applied force. B) Experimental protocol. C) Posterior view of the forearm, with indication of the investigated muscles: Extensor Carpi Radialis (ECR), Extensor Carpi Ulnaris (ECU) and Extensor Digitorum Communis (EDC, monitored to check that its activity is not too high during the contraction of the other muscles and to add a further electrode array). D) Examples of SD test data from a subject: 5 s epochs of selective contractions of ECR and ECU were concatenated; SD channels with IED 25 mm were considered; 3 channels (one over each of the muscles shown in C) were used to design the OSTF.

Figure 7 shows a summary of the tests on experimental SD data. In general, the SCR was lower for larger IED, as the contribution of crosstalk is larger when the filter is less selective. The OSTF provided surrogate signals with larger SCR, with improved results when 3 instead of 2 SD channels were processed. The improvements were statistically significant (Wilcoxon signed rank test, $p<0.05$) considering a fixed IED (including both muscles, otherwise the

observations are too few to make statistical inferences). The mean improvement of the SCR when using the OSTF instead of the SD filter was 1.65 and 2.13 dB, when processing 2 and 3 signals, respectively. The improvements of performances (OSTF using 2 signals versus SD and OSTF using 3 versus 2 channels) were statistically highly significant (Wilcoxon signed rank test, with $p<0.01$) for both the muscles. When considering DD channels (results shown in the Support Material), the mean improvement of the SCR when using the OSTF was again statistically significant for both muscles and equal to about 2 dB (with a marginal, not significant increase when considering 3 instead of 2 signals to design the OSTF).

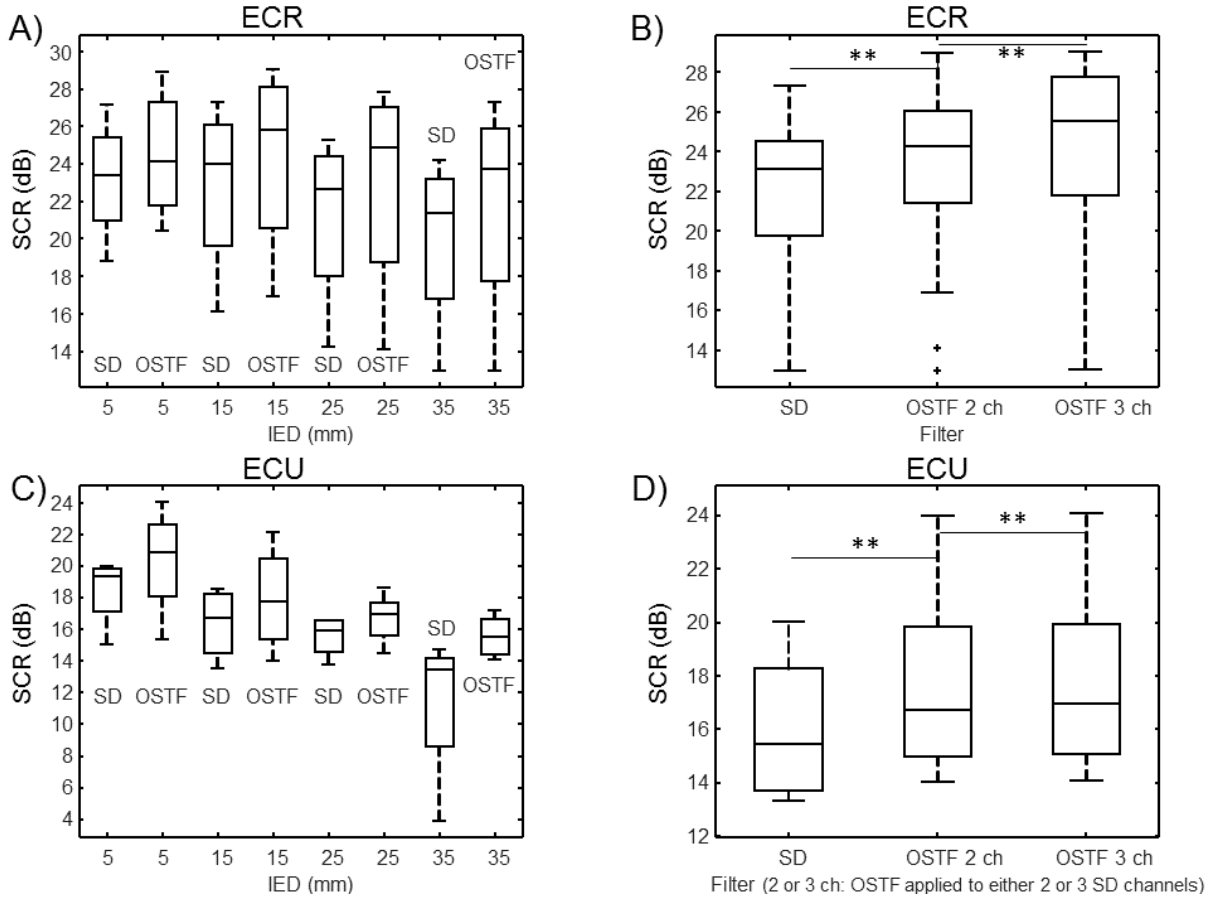

Figure 7. Summary of tests on experimental SD data (4 subjects, 32 contractions each, 8 of which were used for training). ECR is considered in A) and B), ECU in C) and D). A) and C): distribution of SCR (median, quartiles and range) of SD and surrogates considering different IEDs. B) and D): SCR of SD and surrogates obtained using either 2 or 3 SD channels (over ECR and ECU in the first case, adding also the channel over EDC in the second). Some statistically significant differences are indicated with ** ($p<0.01$).

Discussion

Crosstalk is one of the main open problems in surface EMG research and applications [1-5,12,30]. Research studies usually use high-density detection systems and selective filters to reduce the EMG from muscles close to the one of interest. However, selective filters (by

definition) detect small contributions both from other muscles (reducing crosstalk) and from the one of interest, thus providing limited information from the investigated muscle. Moreover, the level of selectivity depends on the specific anatomy [6], so that it is not possible to define the optimal filter in terms of selectivity without adapting to the condition at hand. In applicative studies, a few electrodes with large contact surface and great IED are usually used, with the attempt to record EMG from a big region representing the activity of the whole muscle of interest. However, in this way, the recording is prone to crosstalk as the signal includes also the EMG from nearby muscles.

In this paper, a new approach is discussed to design a filter adapted to the specific application, which was called optimal spatio-temporal filter (OSTF). It is proposed to improve the signal to crosstalk ratio (SCR). The method adapts to the condition at hand by optimizing the response based on a training set. The solution to the optimization problem defining the OSTF is exact, so that there is the guarantee that the filter is indeed optimal on the training set. The only possible problems concern the stability in cases in which the test signals are much different from the ones used for training. Indeed, the training data provide information about both the anatomy (which is constant if the training signals are recorded in the same conditions as the test data) and the specific EMG, reflecting spatial and temporal MU recruitment (related to the specific force level) and possible peripheral fatigue, and including additive noise. Thus, there is the risk of overfitting, if the OSTF is affected by some properties of the training data that are not found in the test; moreover, there is the possibility that the test signal shows different properties from the training data (e.g., the involvement of additional MUs or the distortion of MUAP shapes due to fatigue). The performances were checked in problematic simulated conditions, in which the training epochs were very short (a few seconds), they were not perfect (contractions were sub-maximal and not selective) and the test data were biased by a great peripheral fatigue (20% reduction of CV). Moreover, the method was tested on experimental data from some forearm muscles, whose contraction was never perfectly selective. Performances of the OSTF were superior to those of the channels (SD or DD) which were processed, with a mean gain of about 2 dB, both considering simulations and experiments. In simulations, the performances of the OSTF were always greater than those of classical filters (Figure 4E). When considering experimental data, the performances of the OSTF were always superior with the exception of 1 and 2 cases using 3 and 2 SD channels, respectively, out of 32 tests (i.e., 4 subjects x 4 IEDs x 2 muscles); in the case of DD, 2 problematic cases were found both when the OSTF processed 2 and 3 channels (the number of tests was 24, i.e., 4 subjects x 3 IEDs x 2 muscles). A visual check of these problematic

conditions suggests that contractions were not much selective in such cases, due to the activity of EDC; moreover, the reduction of performances of the OSTF was small (about 0.1 dB).

The OSTF depends on two parameters that can be tuned to improve the performances: the lag between delayed data and the order of the temporal filter. All tests were performed with delays multiple of 1 and till an order of the temporal filter equal to 10. Considering ideal simulated conditions (in which, only the specific firing pattern and additive noise were different in the training and test sets), the OSTF provided always better performances than classical filters (and this was true even with an order of the temporal filter as high as 50). When all simulated problems were included, occasionally the OSTF provided worst performances than classical filters if the order was larger than 5 (with a decrease of the SCR with respect to the processed channels of about 0.5 dB). Usually, the problems arose if only two channels were processed by the OSTF, when the SNR was high and in conditions in which crosstalk was limited (i.e., small thickness of the fat layer and small IED; notice that, to avoid the risk of overfitting, the OSTF could be avoided in the case in which the effect of crosstalk is limited on the training data). This poor generalization indicates overfitting of the training set, which could be avoided decreasing the order of the temporal filter. The best order for the specific application could be selected by the validation of different OSTFs before application to test data (if this is possible).

Notice that central fatigue, inducing a modulation of the firing rate or MU synchronization [31], is not expected to largely affect the results, as the method is linear and only marginally influenced by the timing of firings. Indeed, the functional to be optimized is affected by the energy of the MUAP trains, which linearly increases with the number of occurrences, but is not related to the specific firing pattern (apart from the amount of phase cancellations, which depends on the firing patterns of different MUs). This observation suggests that the training set could also be constituted by EMG during elicited activity. This could be beneficial as stimulating the contraction of single muscles at a time allows to obtain very selective information. Preliminary simulation tests on using stimulated contractions for the training were encouraging (not shown results). A gradual increase of the amplitude of stimulation is suggested in order that the method can learn different MUAP shapes. However, an experimental protocol including stimulated contractions would be quite time expensive, so that this modality of training was not deepened here and is not suggested in applications (future investigation could be of interest for research studies).

Peripheral fatigue (simulated as a reduction of the CV of all MUs) reduced the performances of the OSTF, as the test set included MUAPs with different morphology than those added up in the training set. However, this problem can be reduced by a time scaling which compensates for CV reduction before application of the OSTF followed by an opposite scaling of the surrogate. When applied to all simulated conditions shown in Figure 4, this method increased the mean SCR of about 0.46 and 1.04 dB, for the application to SD and DD channels, respectively (very significant variation for Wilcoxon signed rank test; not shown results). The correct scaling can be determined monitoring the variation of the mean frequency of the test data (in this way, the method could be applied on single channels; an alternative solution could be based on CV estimation from more channels aligned to the muscle fibers).

Only a few channels were considered in this study (two or three SD or DD). This is the condition usually found in applications in which single channels are used to detect the overall activity of single muscles (e.g., clinical studies, rehabilitation protocols, gait analysis or prosthesis control). However, if more data are processed, the method becomes more stable and performances improve. For example, if channels are placed not only over the muscles of interest, but also between them, the additional information is used by the OSTF to improve the SCR (this was observed both in simulations, Figure 4C, and in experiments, Figures 7B and 7D).

The amplifiers often used in applications provide channels already processed by a spatial filter (e.g., SD channels) without giving to the user access to the monopolar potentials on each electrode. However, monopolar data contain more information than that provided by any other detection channel. This information can be used by the OSTF to get improved performances. For example, some results concerning the OSTF applied to simulated monopolar data (from which common mode was removed) recorded from the same electrodes used to acquire either SD or DD channels are shown in the Support Material. Larger SCRs were obtained than those achieved using SD and DD signals. Notice that monopolar signals can be obtained from SD data if electrodes are connected (i.e., summing different SD channels the difference between the potentials of two arbitrary electrodes can be computed) and if the constraint of zero common mode is imposed [32]. Thus, the same surrogates can be obtained using either monopolar or SD signals, if all electrodes are connected (the only concern is about the increase of random noise due to the linear combination of more channels).

In conclusion, higher performances can be reached using the OSTF if more information is provided (e.g., considering more channels or monopolar instead of SD or DD data). Thus, in research activities in which high-density surface EMG systems are used, the method is expected to get higher performances than those presented here. However, it is noteworthy that the performances of the OSTF are higher than those of classical filters even when considering the few channels usually used in applications. Moreover, the method is fairly stable to possible problems in the training and test data (if the order of the temporal filter is about 4 or 5).

Many applications of the OSTF are suggested. The representative examples shown in Figure 5 indicate that the OSTF may reduce the bias of crosstalk in the estimation of CV and force level. Further applications are suggested in movement analysis or in the identification of muscle synergies. The method could be employed also in problems not directly related to crosstalk. For example, in prosthesis control, a motor task could involve more muscles in synergy. In that case, the surrogate signal that identifies such a task optimally (from an energetic viewpoint) is the one with maximal energy during its execution and minimal energy otherwise (during rest or the execution of other tasks). Thus, different OSTFs could be applied to emphasize the signal during the execution of each of the tasks of interest, in order to facilitate their identification.

A generalization of the method can also be proposed in the future. The SCR was here defined as a ratio of energetic norms, but other norms could be used: for example, the L_1 norm. Increasing the ratio between the L_1 norm of the signal and of crosstalk allows to select a filter that reduces the relative mean rectified amplitude of the interference with respect to that of the signal (instead of its energy, as in the case of the filter discussed here). Notice that an energetic functional (as that considered here) gives much importance to samples with high amplitude (usually related to the activity of the muscle of interest) and tolerates errors with small amplitude (usually reflecting crosstalk). Thus, the OSTF here considered is expected to increase the SCR by emphasizing the signal, more than reducing crosstalk. On the other hand, optimizing a functional including L_1 measurements of the signal and noise norms, it is expected that the amplitude of crosstalk can be further reduced than when applying the OSTF.

The OSTF is related to methods introduced in other fields. As indicated in the Methods section, the optimization problem can be solved using the same theoretical ideas involved in Linear Discriminant Analysis. Moreover, similar filtering approaches were introduced in the study of electroencephalogram (EEG), e.g., to focus better on the activity of specific sources

reducing the EEG from nearby cortical neurons [33] or to decode the intention of movement (OSF [21] or common spatial patterns [34] applied to BCI applications).

Conclusions

This paper introduces a filter designed to reduce crosstalk in surface EMG. It is adaptive and optimal on a training set. Its performances on simulated and experimental test data are greater than those of classical spatial filters. The method works also if a few channels are considered (even a single channel over each muscle of interest), showing to be potentially useful not only in research studies employing high-density systems, but also in applications in which a few, not selective recordings are considered.

Acknowledgments: Experimental data were provided by LISiN (Laboratorio di Ingegneria del Sistema Neuromuscolare e della riabilitazione motoria, Turin, Italy). They were recorded by Dr. E. Sosso, working under my supervision and participating to an Erasmus European exchange project involving the laboratories CREB (Centre de Recerca en Enginyeria Biomèdica, Barcelona, Spain) and LISiN.

References

[1] Hug F 2011 Can muscle coordination be precisely studied by surface electromyography? J Electromyogr Kinesiol, **21** 1–12.

[2] Mitchell Barr K, Miller AL and Chapin KB 2010 Surface electromyography does not accurately reflect rectus femoris activity during gait: Impact of speed and crouch on vasti-to-rectus crosstalk, Gait & Posture **32** 363–8.

[3] Yong-Ku Kong, Hallbeck MS and Myung-Chul Jung 2010 Crosstalk effect on surface electromyogram of the forearm flexors during a static grip task, J Electromyogr Kinesiol 20 1223–9.

[4] Jiang N, Englehart KB and Parker PA 2009 Extracting simultaneous and proportional neural control information for multiple-DOF prostheses from the surface electromyographic signal, IEEE Trans Biomed Eng **56** 1070-80

[5] Mezzarane RA and Kohn AF 2009 A method to estimate EMG crosstalk between two muscles based on the silent period following an H-reflex, Med Eng Phys. **31** 1331–6.

[6] Mesin L, Smith S, Hugo S, Viljoen S and Hanekom T 2009 Effect of spatial filtering on crosstalk reduction in surface EMG recordings. Med Eng Phys **31** 374–83.

[7] Stoykov NS, Lowery MM and Kuiken TA 2005 A finite-element analysis of the effect of muscle insulation and shielding on the surface EMG signal. IEEE Trans Biomed Eng. **52** 117-21.

[8] Mesin L 2008 Simulation of surface EMG signals for a multilayer volume conductor with a superficial bone or blood vessel. IEEE Trans Biomed Eng. **55** 1647-57

[9] Lowery MM, Stoykov NS, Taflove A and Kuiken TA 2002 A multiplelayer finite-element model of the surface EMG signal, IEEE Trans. Biomed. Eng. **49** 446–454.

[10] Lowery MM, Stoykov NS, Dewald JP and Kuiken TA 2004 Volume conduction in an anatomically based surface EMG model, IEEE Trans. Biomed. Eng. **51** 2138–47.

[11] De Luca CJ, Kuznetsov M, Donald Gilmore L and Roy SH 2012 Inter-electrode spacing of surface EMG sensors: Reduction of crosstalk contamination during voluntary contractions, J Biomechanics **45** 555–61.

[12] Farina D, Merletti R, Indino B, Nazzaro M and Pozzo M 2002 Surface EMG crosstalk between knee extensor muscles: experimental and model results. Muscle Nerve **26** 681-95.

[13] Farina D, Arendt-Nielsen L, Merletti R, Indino B and Graven-Nielsen T 2003 Selectivity of spatial filters for surface EMG detection from the tibialis anterior muscle, IEEE Trans. Biomed. Eng. **50** 354–364.

[14] Farina D, Févotte C, Doncarli C and Merletti R 2004 Blind separation of linear instantaneous mixtures of nonstationary surface myoelectric signals. IEEE Trans Biomed Eng. **51** 1555-67.

[15] Merletti R, De Luca CJ and Sathyan D 1994 Electrically evoked myoelectric signals in back muscles: Effect of side dominance, J. Appl. Physiol., **77** 2104–14.

[16] Solomonow M, Baratta R, Bernardi M, Zhou B, Lu Y, Zhu M and Acierno S 1994 Surface and wire EMG crosstalk in neighbouring muscles. J Electromyogr Kinesiol **4** 131–42.

[17] Campanini I, Merlo A, Degola P, Merletti R, Vezzosi G and Farina D 2007 Effect of electrode location on EMG signal envelope in leg muscles during gait, J Electromyogr Kinesiol **17** 515–26.

[18] Dimitrova NA, Dimitrov GV and Nikitin OA 2002 Neither high-pass filtering nor mathematical differentiation of the EMG signals can considerably reduce cross-talk, J Electromyogr Kinesiol, **12** 235-46.

[19] Lowery MM, Stoykov NS and Kuiken TA 2003 A simulation study to examine the use of cross-correlation as an estimate of surface EMG cross talk, Journal of Applied Physiology **94** 1324-34.

[20] Mesin L 2015 Real time identification of active regions in muscles from high density surface electromyogram. Comput Biol Med. **56** 37-50.

[21] Niazi IK, Jiang N, Tiberghien O, Nielsen JF, Dremstrup K and Farina D 2011 Detection of movement intention from single-trial movement-related cortical potentials. J Neural Eng. **8** 066009.

[22] Welling M 2005 Fisher linear discriminant analysis, Department of Computer Science, University of Toronto.

[23] Fletcher R 1987 Practical methods of optimization, John Wiley & Sons.

[24] Farina D, Mesin L, Martina S and Merletti R 2004b A surface EMG generation model with multilayer cylindrical description of the volume conductor. IEEE Trans Biomed Eng. **51** 415-26.

[25] Fuglevand AJ, Winter DA and Patla AE 1993 Models of recruitment and rate coding organization in motor-unit pools, J. Neurophysiol. **70** 2470-88.

[26] Andreassen S and Arendt-Nielsen L 1987 Muscle fiber conduction velocity in motor units of the human anterior tibial muscle: A new size principle parameter, J. Physiol. **391** 561-571.

[27] Jochumsen M, Niazi IK, Mrachacz-Kersting N, Farina D and Dremstrup K 2013 Detection and classification of movement-related cortical potentials associated with task force and speed. J Neural Eng. **10** 056015

[28] Jochumsen M, Niazi IK, Mrachacz-Kersting N, Jiang N, Farina D and Dremstrup K 2015 Comparison of spatial filters and features for the detection and classification of movement-related cortical potentials in healthy individuals and stroke patients. J Neural Eng. **12** 056003.

[29] McGill KC and Dorfman LJ 1984 High resolution alignment of sampled waveforms, IEEE Trans. Biomed. Eng. **31** 462-70.

[30] Ison M and Artemiadis P 2014 The role of muscle synergies in myoelectric control: trends and challenges for simultaneous multifunction control. J Neural Eng. **11** 051001.

[31] Mesin L, Dardanello D, Rainoldi A and Boccia G 2016 Motor unit firing rates and synchronisation affect the fractal dimension of simulated surface electromyogram during isometric/isotonic contraction of vastus lateralis muscle. Med Eng Phys. **38** 1530-3.

[32] Mesin L 2009 Estimation of monopolar signals from sphincter muscles and removal of common mode interference, Biomed. Sig. Proc. and Control **4** 37-48.

[33] Van Veen BD, van Drongelen W, Yuchtman M and Suzuki A 1997 Localization of brain electrical activity via linearly constrained minimum variance spatial filtering, IEEE Trans Biomed Eng **44** 867–880.

[34] Sannelli C, Vidaurre C, Müller KR and Blankertz B 2016 Ensembles of adaptive spatial filters increase BCI performance: an online evaluation. J Neural Eng. **13** 046003.

5

Journal of Neural Engineering

SUPPORT MATERIAL

Optimal Spatio-Temporal Filter for the Reduction of Crosstalk in Surface Electromyogram

Luca Mesin[1]

[1] *Mathematical Biology and Physiology, Dipartimento di Elettronica e Telecomunicazioni, Politecnico di Torino, Corso Duca degli Abruzzi 24, 10129, Turin, Italy*

Results in addition to those shown in the paper are here presented. The first results concern additional tests in simulations, the last was obtained from experimental data.

Additional results from tests on simulations

The shown figures I-IV are similar to figures 2-5 of the main part of the paper (to make this document self-contained, some descriptions already discussed in the paper are here repeated). However, instead of using the SD or DD channels (as in the main part of the paper), here the OSTF is applied to the monopolar data from the same electrodes considered to detect the SD or DD channels (equivalent results can be obtained processing SD signals if the electrodes are connected, as indicated in the Discussion of the main paper).

Figure I shows an example of ideal application. Training data were obtained by an alternative selective activation of duration of 1 s of either of the two muscles with force levels of 20, 40, 60 or 80% MVC. Test data were simulated considering again the same activation protocol, but with each contraction lasting 5 s. The SD and DD channels were obtained considering either 2 or 3 noisy monopolar EMGs detected from electrodes aligned to the muscle fibres, with IED 5 mm. Notice the difference with respect to the simulations considered in the paper: here, Gaussian white noise with a specific SNR was added to monopolar data; then they were filtered (anti-aliasing filter with cutoff frequency of 500 Hz, Chebyshev Type II filter of order 6 with 20 dB attenuation in the stop-band, used in both directions to remove the phase) and SD or DD channels were obtained from them; in this way, the detection of noisy monopolar

EMGs was simulated. On the other hand, in the main part of the paper, SD and DD signals were simulated and then corrupted by colored Gaussian noise with a SNR measured in terms of the energy of the SD and DD (not monopolar) data; in this way, the detection of noisy SD and DD data was simulated.

Each channel was placed over one of the two muscles, with a distance of 20 mm between the centers of the spatial filters and the midline between the two muscles. Surrogate signals were obtained considering the same monopolar data (either 4 or 6 monopolar signals, to compare with SD and DD detection, respectively). Notice that the SCR (defined as the ratio between the power of the signal during the activation and the relaxation of the muscle of interest) is larger for the surrogate channel than for the classical spatial filters. Moreover, it was larger than that shown in Figure 2 of the paper in which two SD or two DD channels were considered (instead of either 4 or 6 monopolar data, respectively).

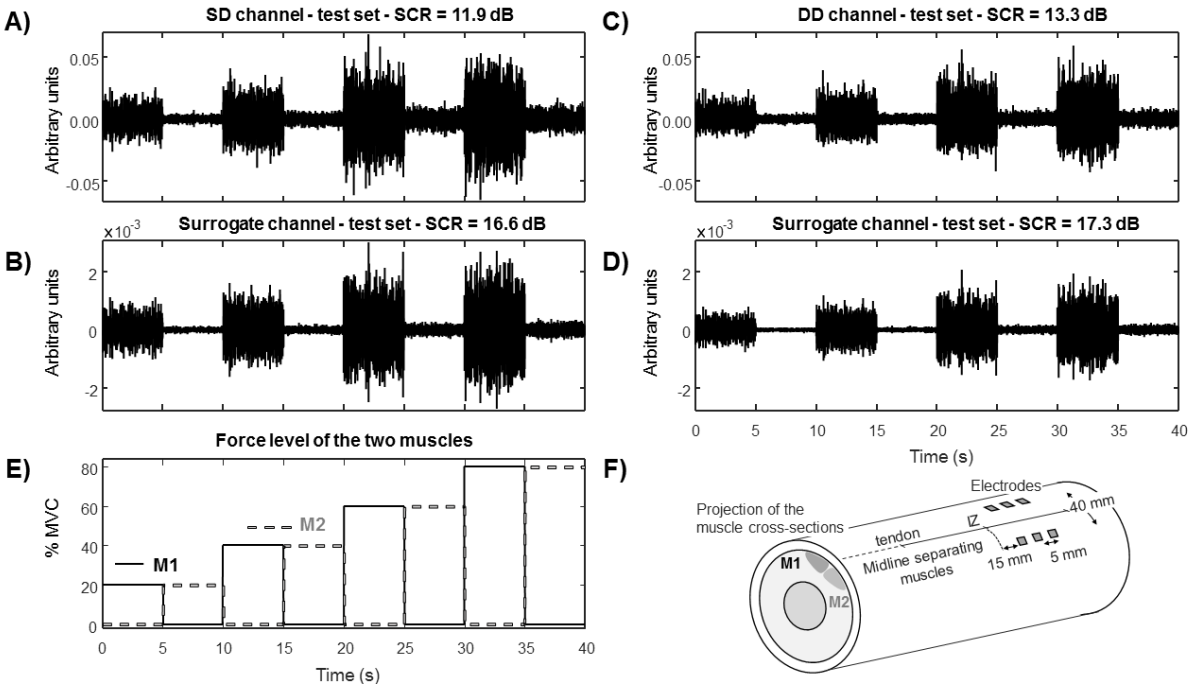

Figure I. Example of single differential (SD), double differential (DD) and surrogate data (volume conductor with thickness of fat layer equal to 7 mm; noise with SNR of 30 dB was added on monopolar data before computing SD, DD and surrogates). Training set was equivalent to the test dataset (it was only 4 times shorter). A) SD data with indication of the signal to crosstalk ratio (SCR); the pair of electrodes closer to the IZ were considered. B) Surrogate signal obtained from the same 4 monopolar data used to detect the SD EMGs over the two muscles, with order for the temporal filter equal to 5. C) DD data. D) Surrogate signal obtained considering the 6 electrodes used to detect DD channels over the two muscles. E) Force level of the two muscles during the generation of the test dataset. F) Representation of the volume conductor and electrodes considered.

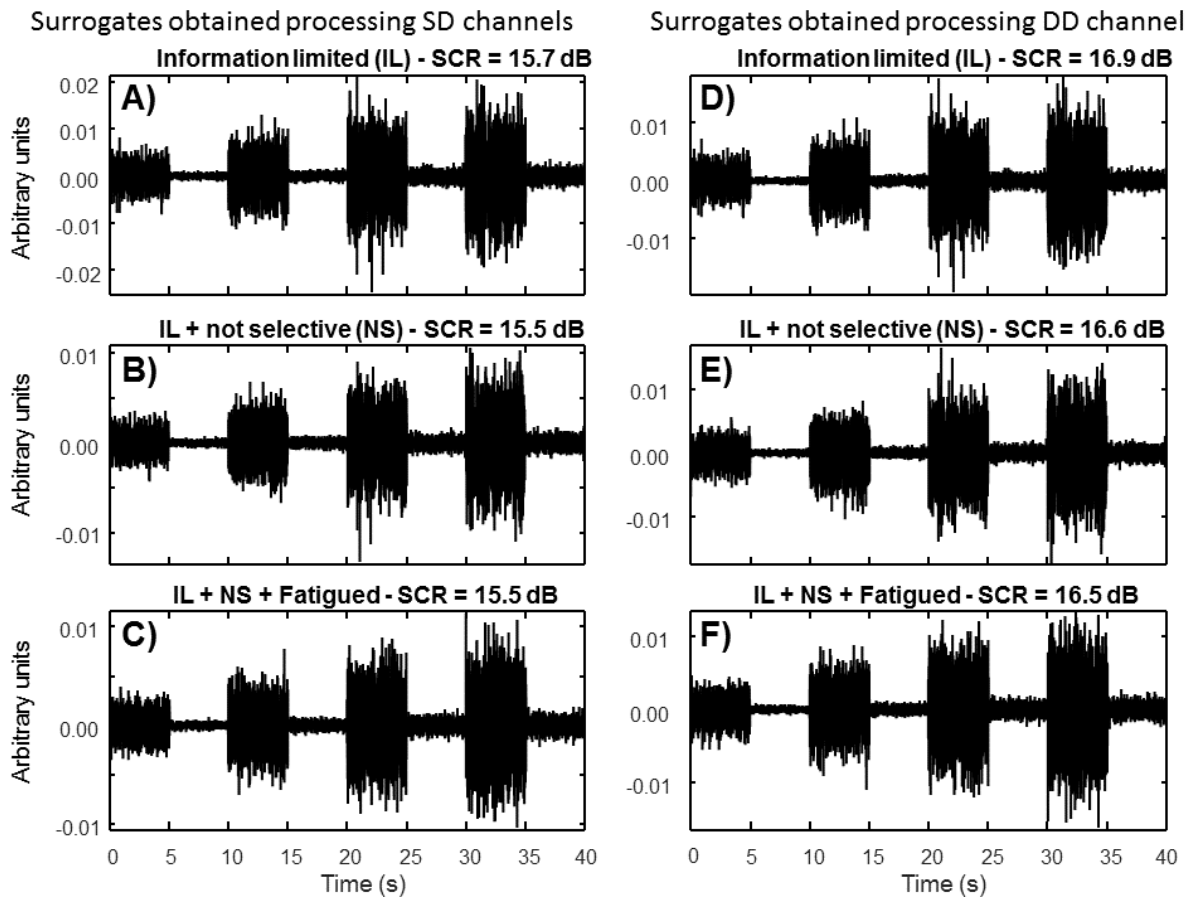

Figure II. Examples of surrogate data obtained considering the same configuration as in Figure I, but including different problems and using an order for the temporal filter equal to 4. A), B), C) Four monopolar data are considered (as in 2B). D), E), F) Six monopolar signals are considered (as in 2D). A), D) Only force levels of 20% and 40% of maximal voluntary contraction (MVC) were considered for the training set. B), E) In addition to the limited information, in the training set the contractions were not selective, but they included a contraction of the other muscle at 5% MVC. C), F) In addition to the previous problems, the test data showed myoelectric fatigue (20% reduction of muscle fiber conduction velocity).

Figure II shows some examples of results obtained in equivalent conditions as in Figure I, but considering some problems in the training or in the test data. In Figure II-A, the effect of limited information in the training set is considered: only contraction levels of 20 and 40% MVC were considered in the training set. As the recruitment threshold of the largest MU was 60% MVC, only some MUs were used to build the training data. In Figure II-B, in addition to the limited information, a further problem was added: contractions used for the training were not perfectly selective, but a contraction with level either 5 or 10% MVC of the muscle assumed to be silent was included during a contraction of either 20 or 40% MVC, respectively, of the muscle assumed to be active. Figure II-C includes a further problem, in addition to the previous ones: the muscle is fatigued during the test, with a reduction of

muscle fiber CV of 20%. Notice that performances decrease as problems are included in the training and test set. Comparing the results with Figure 3 of the paper, the performances are better when compared with those obtained using SD data and are equivalent when considering DD data.

Figure III shows a summary of the results of many simulations. The following parameters were changed across different simulations:

1. fat layer thickness (either 3 or 7 mm),
2. IED (5 or 10 mm),
3. SNR of the monopolar channels (considering additive Gaussian white noise with SNR of either 20 or 30 dB),
4. number of spatial filters, either 2 or 3, with the latter case indicating that an additional channel was located over the midline between the two muscles (the spatial filters over the muscles were always at 20 mm from the midline).

The order of the temporal filter of the OSTF was 4, which allows to get stable results in all conditions. All cases discussed above (and shown in Figure I and II) were considered: ideal condition in which training data included perfectly selective contractions at different force levels ranging among 20 to 80% MVC and test data were generated considering the same MUAPs as for the training data; limited information in the training data (up to a force level of 40% MVC); limited information and not selective contractions used for the training data; same training data as in the latter case, but considering test data showing myoelectric manifestation of peripheral fatigue. General results are as expected (all following indications are statistically significant for Wilcoxon signed rank test, with $p<0.01$): performances of the OSTF decrease (i.e., a lower SCR is obtained) when problems on training or test data are included; performances of all methods decrease by increasing the fat layer thickness and by decreasing the SNR; performances of the OSTF increase when including an additional array of electrodes over the midline separating the two muscles. Performances of all filters increase also when IED is larger: this is in line to what expected for the OSTF, as less correlated information are included in the monopolar signals when considering a larger IED, so that a better estimation of the global activation of the muscle of interest is obtained; on the other hand, SD and DD filters should be more selective considering a smaller IED, with an expected benefit on reducing crosstalk. Further tests showed that such a benefit is obtained only considering very clean monopolar signals (SNR around 40 dB); in the simulated conditions, considering a very selective filter, like DD with small IED, decreased the signal

component and kept a great amount of noise (notice that in III-D the median performance of DD is even worse than that of SD with SNR of 20 dB).

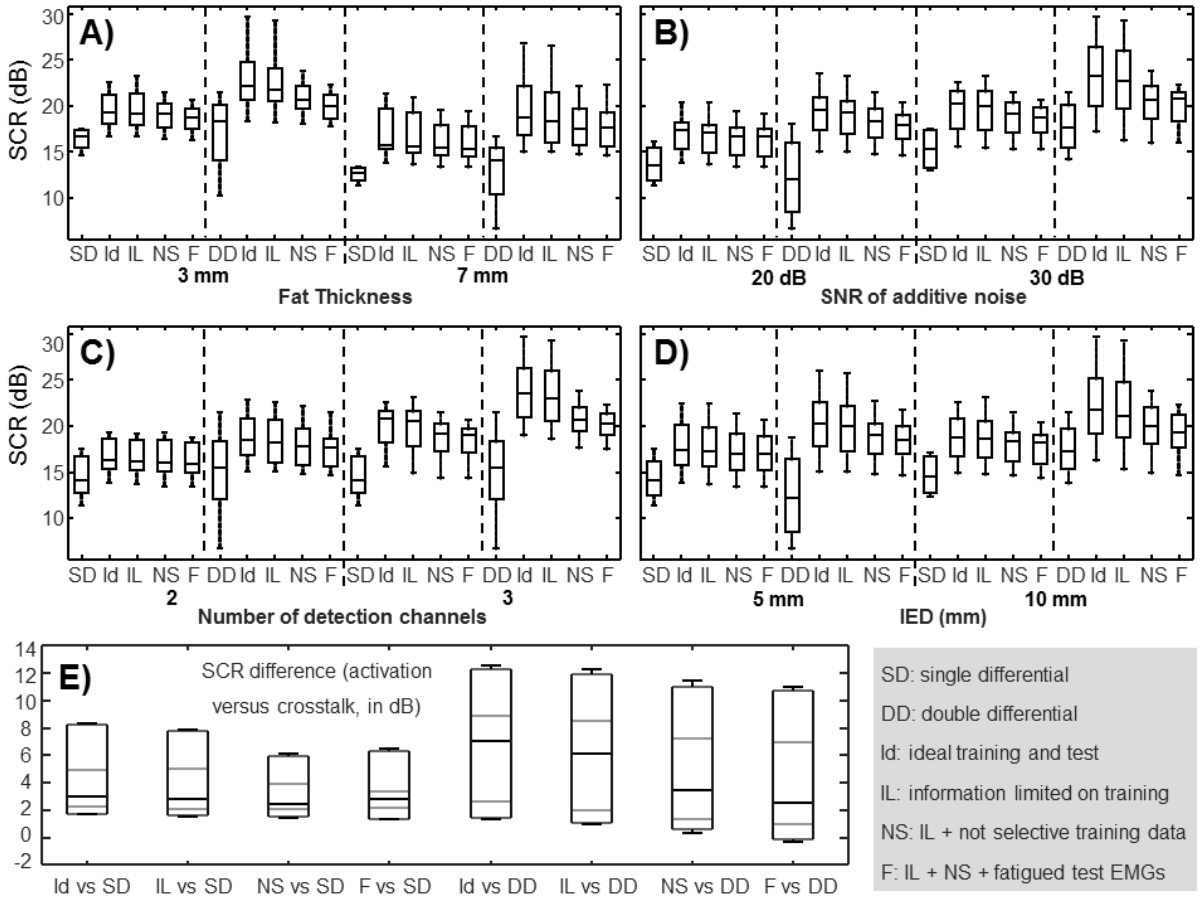

Figure III. Summary of many simulations (order of the temporal filter equal to 4). The following parameters were changed across simulations: fat layer thickness (either 3 or 7 mm), IED (5 or 10 mm), SNR of the monopolar channels (20 or 30 dB), number of spatial filters (either 2 or 3, with 3 indicating that electrodes were placed also over the midline between the two muscles). Ten realizations of noise were considered for each simulated condition. SD or DD channels were simulated. Surrogates were computed considering the same monopolar channels considered to record either SD or DD data, in either ideal conditions (training and test data with equivalent properties) or including the problems also shown in Figure II. Data were pooled, showing the effect of different parameters: A) fat thickness, B) noise level, C) number of channels, D) IED. E) Distribution of differences between SCR obtained using surrogates or either SD or DD (range, median and percentiles of percentages 5, 25, 75, 95).

For the interpretation of these results (and also of those shown in the previous figures), notice that the SNR considered here should be interpreted differently from the one of the signals studied in the paper. Indeed, in the paper, as mentioned above, the SNR was defined on either the SD or DD signals; on the other hand, here it indicates the amount of noise in the monopolar data. The SNR of the SD and DD channels obtained filtering noisy monopolar data should be computed studying the variation of the energy of the signal and of the noise

when applying the spatial filters. For example, considering a fat layer of 7 mm, the RMSs of the SD are about the 38% or 71% of that of monopolar data, considering IED of either 5 or 10 mm, respectively; the RMSs of the DD are about the 23% or 78% of that of monopolar data, considering again IED of either 5 or 10 mm, respectively; on the other hand, the energy of the noise included in the SD and DD channels obtained from the monopolar data are 2 and 4 times those of the noise added to the original signals (as the variance of independent Gaussian noise increases linearly with the number of signals that are combined). Thus, when spatial filters are built from recorded monopolar data, the SNR of the obtained signal depends on physical and anatomical properties; these considerations limit the possibility of making a direct comparison between the results shown here and those reported in the paper. However, considering only the effect of crosstalk (thus, with a very high SNR), the additional information contained in monopolar data allows to increase the performances of the OSTF. Indeed, notice that, using monopolar data, the OSTF makes the linear combination of more signals than using SD or DD channels (there are twice the number of SD channels and 3 times the number of DD signals). Thus, there is the possibility of fitting better the training data (but with the risk of making also overfitting; for this reason, the order of the temporal filter was 4 and not 5 as for the results shown in the paper). As shown in III-E, the performances of surrogates were always greater than those of SD and DD filters, with a single exception for the comparison between DD and surrogate obtained from the most problematic data (limited information and not selective training data, fatigued test EMGs): DD performances overcame those of the OSTF in about 9% of cases. All of these cases were characterized by the following conditions: small fat layer thickness and large IED; moreover, most cases included a small noise level and only 2 arrays of electrodes (thus, DD can have better performances only if crosstalk and noise are small and the OSTF is trained on data containing problems and applied to test signals which are quite different from the training set). Notice that considering the compensation of CV reduction (mentioned in the Discussion section of the paper), the performances of the OSTF improved and were always better than those of SD and DD.

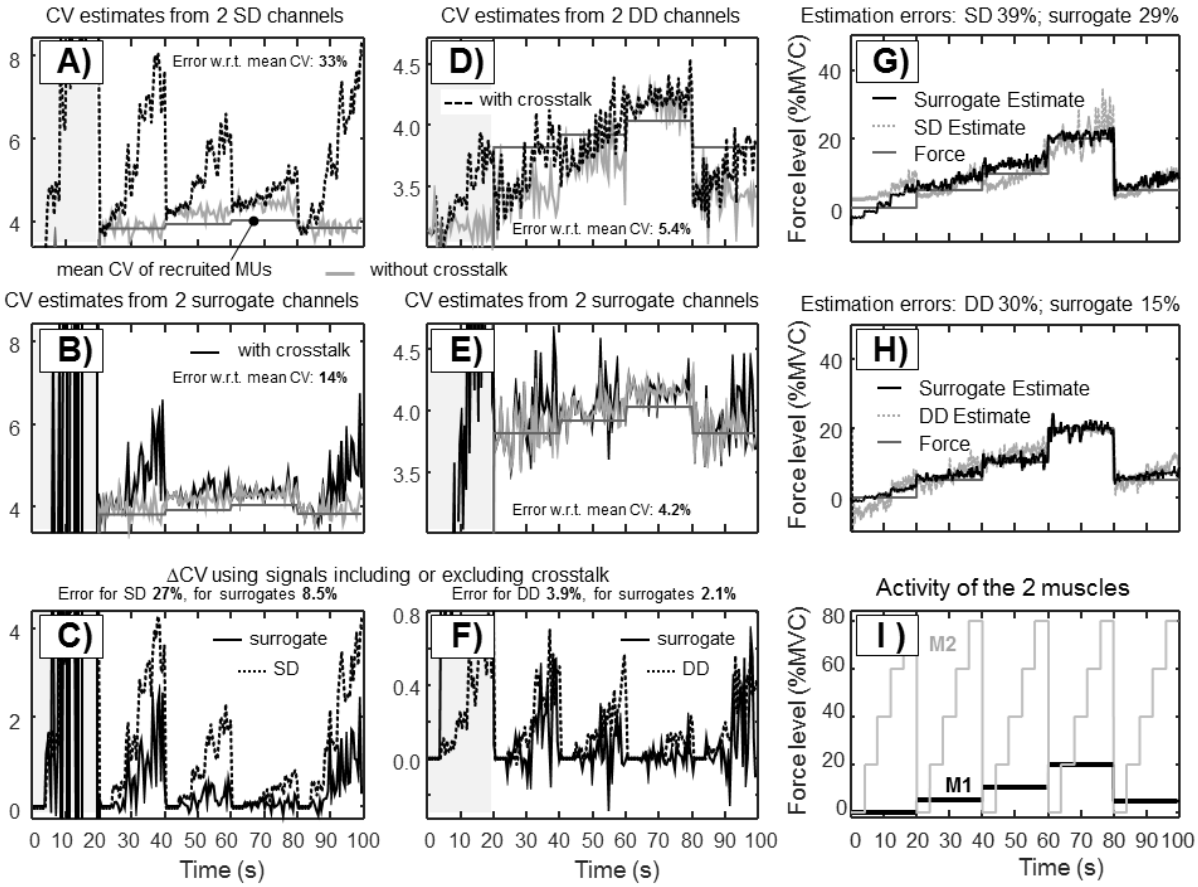

Figure IV. Examples of applications (with fat thickness 7 mm, SNR 30 dB, ideal training and order of the temporal filter equal to 10): A)-F) CV estimation; G), H) force level estimation. A) CV estimation using epochs of 0.5 s of two SD channels from 3 electrodes aligned to the fibers, with 5 mm of IED and placed over the first muscle (M1), at 20 mm from the midline separating the two muscles. Crosstalk was either included or not. B) Same as A), but considering surrogates computed from an ideal training set, using 3 arrays of the same electrodes used to simulate the SD filter (the first array as in A, the second over the midline, the third over M2, symmetrical to the first with respect to the midline). C) Difference between the CV computed either including or excluding crosstalk. D) Same as A), but considering DD channels. E) Same as B), but using arrays of 4 electrodes (needed to acquire 2 DD channels). F) Same as C), but using data shown in D) and E). G) Estimation of force level using the envelope of SD and corresponding surrogate, with a quadratic model. H) Estimation of force level using the envelope of DD and surrogate. I) Force levels of the two muscles over time.

Figure IV shows applications to CV and force level estimation. Both estimates are biased by crosstalk, mainly when the muscle of interest has a low level of contraction. The simulated force level of the muscle of interest was between 0 and 20% MVC, whereas that of the other muscle ranged between 20 and 80% MVC. In the training set, the muscles were activated selectively, whereas the two muscles were active together during the test (as shown in IV-I). CV was computed with the spectral matching algorithm, considering either a pair of SD or DD filters, aligned to the muscle fibers and placed over the muscle of interest (at 20 mm from

the midline), or using the OSTF (3 arrays were used, 2 over the muscles and 1 on the midline separating them). The OSTF was trained considering monopolar EMGs from electrodes closer to the IZ; it was then applied to the test data from electrodes either closer to the IZ or to the tendon, obtaining the ideally delayed signals to which the spectral matching algorithm was applied. The estimates were computed from data either including or excluding crosstalk. Moreover, the mean CV of active MUs of the muscle of interest (weighted by the sizes of the MUs) was computed as a further reference. CV estimated when the muscle of interest was not contracted (left portions of Figure IVA-F) are not reliable. The other values are affected by a larger bias when the force level of the muscle of interest is lower and that of the other muscle is greater. However, the OSTF allows to get a better estimation of CV, both when compared to the mean CV of active MUs and with the one computed from crosstalk-free data.

Force estimation is shown in Figure IV G-H, considering the same signals as before, using the portion of the electrode grid closest to the IZ. Given the signal of interest (using either SD, or DD, or the two surrogates from the OSTFs), the envelope was computed (low-pass filtered absolute value, with cutoff frequency of 3 Hz, Chebychev type II filter of order 6, processing in both directions to remove the phase). Then, a quadratic model was fit to the training data to estimate the force level. The model was then applied to the test data. Notice that SD and DD show a large bias, due to the activity of the other muscle.

Different orders of the temporal filter of the OSTF were considered. In the figure, the order of the filter was equal to 10. Considering an order of 4 (which allows to get stable estimates also in case of problems on training or test data), the performances were still greater than those obtained using SD and DD. Specifically, considering the surrogate obtained using either arrays of 2 or 3 electrodes, the following performances were obtained: error of CV when including versus excluding crosstalk about 16 and 2.5%, respectively (these performances are larger than those shown in Figure IV for SD and DD, which show errors of 27 and 3.9%, respectively); error in estimating mean CV about 20 and 4.4%, respectively (with SD and DD, the errors shown in Figure IV are 33 and 5.4%, respectively); in force estimation, using arrays of 2 and 3 electrodes, the error was about 30 and 16%, respectively (using SD and DD, the errors were 39 and 30%).

Additional results from tests on experimental data

Figures V is similar to Figures 7 of the main paper, but here DD data are considered instead of SD. Notice that the SCR did not decrease by increasing the IED, as happened for SD channels. This is probably due to the large reduction of propagating components using a

selective double differentiation, which was lower when the IED increased. Moreover, adding a third electrode array (placed over the EDC) provided only a marginal, not significant improvement of the performances of the OSTF. Possibly, this is due to the activity of EDC, which provided different contributions to the contractions, making them more or less selective. Thus, the information recorded over it with the selective DD filter was not much reliable and largely discarded by the OSTF.

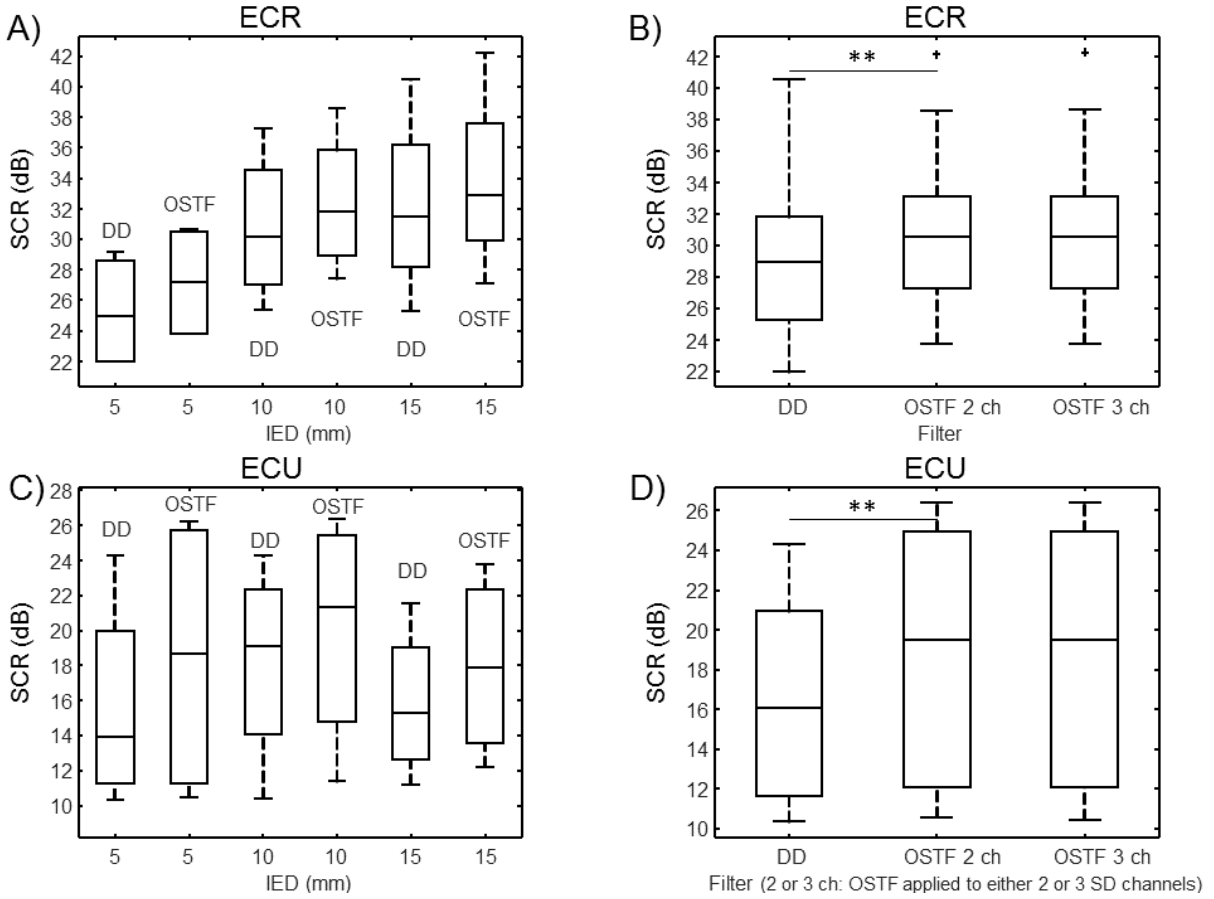

Figure V. Summary of tests on experimental DD data (4 subjects, 32 contractions each, 8 of which were used for training). ECR is considered in A) and B), ECU in C) and D). A) and C): distribution of SCR (median, quartiles and range, outliers shown individually) of SD and surrogates considering different IED. B) and D): SCR of SD and surrogates obtained using either 2 or 3 DD channels (over ECR and ECU in the first case, adding also the channel over EDC in the second). Some statistically significant differences are indicated with ** ($p<0.01$).